Published in final edited form as:

Artif Cells Nanomed Biotechnol. 2018 ; 46(SUP3): S434–S447. doi:10.1080/21691401.2018.1499660.

Comparison of covalently and physically cross-linked collagen hydrogels on mediating vascular network formation for engineering adipose tissue

Chia-Hui Chuang[a], **Ruei-Zeng Lin**[b,c], **Juan M. Melero-Martin**[b,c,d], and **Ying-Chieh Chen**[e]

[a]Department of Applied Science, National Tsing-Hua University, Hsinchu 30013, Taiwan, R. O. C..

[b]Department of Cardiac Surgery, Boston Children's Hospital, Harvard Medical School, Boston, Massachusetts 02115, USA.

[c]Department of Surgery, Harvard Medical School, Boston, Massachusetts 02115, USA.

[d]Harvard Stem Cell Institute, Cambridge, Massachusetts 02138, USA.

[e]Department of Materials Science and Engineering, National Tsing-Hua University, Hsinchu 30013, Taiwan, R. O. C.

Abstract

Timely tissue vascularization and integration of engineered tissues into a patient plays an important role in the successful translation of engineered tissues into clinically relevant therapies. To decrease the time needed to vascularize an engineered adipose tissue, suitable local microenvironments provided by hydrogels to support cell-based functional vascular network formation have been investigated. Using the same biomolecule in solution two types of hydrogels can be obtained: a "physical hydrogel" which is thermal-induced self-assemble fibril initiation and growth, due to amino and carboxyl telopeptides on collagen chains, and a "chemical hydrogel" which results from the covalently cross-linking of the side chains induced by one step enzyme mediation in aqueous solution. In this paper, we compare the capability of engineering vascular network and large-sized vascularized adipose tissue *in vivo* in different types of collagen hydrogels, physical and chemical crosslinking. The relationships between vascular network formation and hydrogel properties for the two types of hydrogels are discussed. Finally, we successfully engineered a vascularized adipose tissue construct (~877.6 adipocytes/mm^2; 94% area of a construct) in the absence of exogenous cytokines in chemical covalently crosslinking cell-laden hydrogel. These results show manipulating the polymerized methods of a hydrogel could not only modulate vascular network formation, but also regenerate adipose tissue *in vivo*.

Keywords

adipose tissue engineering; vascular network; Endothelial colony forming cells; hydrogel

1. Introduction

Current clinical treatments for large-volume adipose tissue reconstruction, specifically for breast tissue, rely on transplanting autologous tissue flaps or relocating autologous fat (i.e.

so-called lipofilling) as a free graft [1]. The major drawback for these techniques is the unpredictable resorption rate of newly-formed fat tissue due to the delayed vascularization associated with subsequent cell necrosis, fibrosis, and graft volume loss at the recipient site [2]. After the procedure, resorption generally occurs within 4–6 months [3], and the rate of resorption can reach 90 % in experimental studies but is limited to 40–60 % in clinical trials [4]. Although lipofilling is well accepted in daily clinical treatment, a high percentage and variable amount of fat resorption reduces the clinical efficacy of this procedure and often results in the need for further grafting [4]. In this context, integrating functional vasculature may offer valuable solutions for engineering larger and functional constructs, in addition to further enhancing adipose tissue engraftment and maintenance, in which nutrient and oxygen diffusion is limited by distance and metabolism after transplantation [2, 5].

The importance of vascularization is widely recognized and cannot be overstated. The methods available for achieving vascularization of engineered tissues over time are limited and depend on the scaffolds/hydrogels, cells, and exogenous growth factors/cytokines used. The most common strategy is the use of a suitable hydrogel as scaffold incorporated with growth factors including vascular endothelial growth factors (VEGF) and fibroblast growth factors (FGF-1/2) [6, 7, 8]. This mimics the natural extracellular matrix (ECM) and could also provide timely, necessary nutrients and oxygen needed for cells embedded in the whole tissue construct through a self-assembling vascular network [9, 10, 11, 12]. The drawback associated with exogenous growth factors is that they do not stimulate vascularization over time when applied in large grafts. Therefore, co-cultures of mesenchymal stem cells (MSC) and endothelial cells (EC) have been used as a model of vasculogenesis, because MSC act as pericytes that provide paracrine cell signaling over time to promote endothelial-mediated vessel formation and maturation that successfully shorten the time that is needed to vascularize an engineered tissue [13, 14, 15, 16, 17]. Endothelial colony-forming cells (ECFC), a subpopulation of endothelial progenitor cells, are readily attainable, easily isolated, high proliferative, so are a promising source of EC for future vascular therapeutic applications[13, 14, 15, 16, 17].

Pure collagen hydrogels are an ideal injectable material in EC/MSC-mediated vascular network formation (80–100 lumens/mm^2) because of their natural biocompatibility, similarity to native ECM, and self-assembly gelation through physical crosslinking. Varying the collagen concentration of collagen hydrogels formed via physical crosslinking simultaneously alters the stiffness and fibril density of the hydrogel, which has been shown to influence the size and length of endothelial cell-lined lumens [18, 19, 20, 21, 22, 23]. Material properties of physically crosslinked collagen hydrogels are highly interdependent, so it is difficult to understand the effect of a specific material property on blood vessel formation by using this gel system. In addition, its thermal instability, extensive contraction after being mixed with cells, mechanical weakness, and rapid degradation limit its practical applications in vascularized bioengineering of adipose tissues [24, 25]. In response to these limitations, covalently chemical cross-linked collagen hydrogels by conjugating functional groups to collagen molecules or adding cross-linkers has been developed [20, 21, 26]. Previous studies have shown that controlling the crosslinking degree and concentration of various chemicals in chemical crosslinked hydrogels could effectively control endothelial cell-mediated angiogenesis and vasculogenesis *in vitro* [20, 21]. Previous work[26] in our

lab has shown that human ECFC-lined vascular networks can be generated and form functional anastomoses with the existing vasculature to further support the survival of host muscle tissues inside chemical cross-linked collagen-phenolic hydroxyl hydrogels. After 7 days, only fewer perfused blood vessels are observed (<80 lumens/mm^2) and mainly distributed on the border region of the enzymatically cross-linked cell-laden implants comparing with that in physical cross-linked collagen hydrogels due to the slow degradation rate of these chemical cross-linked hydrogels. In most studies, the specific crosslinking method with various crosslinking conditions of hydrogels was chosen to demonstrate the effects of certain material properties on angiogenesis or vasculogenesis. Few studies put emphasis on the effect of crosslinking methods to polymerize hydrogel on EC-pericytes-mediated functional blood vessels formation, and if it's further determine the success for creating large-sized vascularized live tissue *in vivo*. In the current study, we sought to compare collagen hydrogel having somewhat similar chemical and physical characteristics but with different modes of cross-linking. The primary difference between the two-collagen hydrogel materials is the nature of their cross-linking bonds, which also results in diffusion, microstructure and mechanical differences, the covalently cross-linked hydrogel being less permeable, dense and stronger network. The covalently and physical cross-linked collagen hydrogels were systematically examined and compared side by side in capability of engineering functional vascular network and large-size vascularized adipose tissues.

2. Experimental Section

Cell sourcing and culture

ECFCs isolated from human cord blood [14, 27, 28] were cultured in Endothelial Growth Media-2 (EGM-2, Lonza) containing 20 % fetal bovine serum (FBS) (Hyclone), SingleQuots (except for hydrocortisone) (Lonza), and 1 % penicillin/streptomycin (PS, Invitrogen) on collagen type I (5 μg/cm^2, Corning)-coated tissue culture plates. MSCs isolated from human bone marrow [14, 27, 28] were cultured in Mesenchymal Stem Cell Growth Medium (MSCGM)(Lonza) supplemented with 10 % FBS, 1 % PS and 10 ng/mL bFGF (Milipore) on uncoated plates. For experiments, human ECFCs and MSCs were used between passages 8 and 10.

Extraction and characterization of collagen

The pieces of rabbit skin tissue were suspended into 95 % ethanol for 2 minutes, immersed into 0.1M NaOH at 4°C for 24 hours, washed out with distilled water and then poured into 10 % Butanol at 4°C for 24 hours to remove debris and sterile skin tissue. Rabbit collagen (collagen) was extracted with 0.5 M acetic acid at ratio of skin/ acetic acid= 1 g: 9 ml at 4°C for 4 days with continuously shaking. The supernatants of the extracted solutions were collected by centrifugation at 11700 g for 10 minutes at 4°C, and then salted out by adding NaCl to a final concentration of 3 M followed by centrifugation under the same conditions. The pellet was re-dissolved in 0.5 M acetic acid, dialysed against 0.1 M acetic acid for 1 day and against distilled water for another 1 day, and then lyophilised.

Self-assemble collagen hydrogel formation

Freeze-dried collagen was dissolved in 0.05 M acetic acid by stirring at 4°C at indicated concentration. Mixing of collagen solution with suitable amount of cooled calcium- and magnesium-free Dulbecco's phosphate-buffered saline (DPBS) and HEPES in an ice bath, adjusting pH to 7.4–7.6 by 1M NaOH and incubating at 37°C initiated self-assembly gelation process to form a collagen hydrogel.

Synthesis and characterization of collagen-phenolic (collagen-Ph) conjugates

The synthesis of the collagen-Ph conjugate was achieved through conjugating tyramine hydrochloride to collagen. Collagen powder was dissolved at 0.0625 % (w/v) in 0.0125 M HCl aqueous solution at 4°C overnight. Adding morpholinoethanesulfonic acid (MES) to collagen solutions to reach 50 mM and then adjusting pH to 6 by adding 0.1 N NaOH solutions at 4°C. To this solution, 0.135 g of EDC and 0.032 g of NHS were added. The solution was stirred again overnight, dialyzed and freeze-dried to obtain the powder form of collagen-Ph conjugates. Proton nuclear magnetic resonance (^{1}H NMR) spectra were recorded on a Bruker AV-400 (400 MHz) spectrometer at 4°C to characterize the conjugation of phenol compounds of collagen-Ph conjugates (1 mg per ml in D_2O). The absorbance of collagen-Ph conjugates (0.1% (w/w)) was measured at 275 nm using a UV-visible spectrophotometer to determine the phenol content of collagen-Ph conjugates. The phenol content of each sample was estimated by using tyramine hydrochloride solutions with various concentrations as standard curves. In the hemolysis assay, rabbit whole blood and collagen-Ph conjugates (0.1 % (w/v)) were co-incubated in phosphate-buffered saline (PBS) at 37°C under mild shaking for 1 hour. The samples were then centrifuged at 2000 g for 5 minutes, and the concentration of hemoglobin with absorbance at 550 nm in the supernatant was determined by UV-Vis spectroscopy.

Enzymatically cross-linked collagen-Ph hydrogel formation and characterization

80 μl of collagen-Ph aqueous solution was mixed well with adding 10 μl of enzyme horseradish peroxidase (HRP) and hydrogen peroxide (H_2O_2) at the indicated concentrations in DPBS to form 0.15–0.6 %(w/v) collagen-Ph hydrogels. Gelation was initiated by the addition of aqueous hydrogen peroxide solution and determined in starting to go viscous and ending of forming a definite shape. Rheological measurements and swelling tests of the hydrogel formation were performed as described previously[29]. The diffusion test was performed by cross-linking the collagen hydrogel (500 μl) into tubes with 5 mm in diameter at desired conditions. 1 ml trypan blue solution was filled into the bottom of the tube at room temperature. After 24 hours, measuring the height of absorbed trypan blue into the hydrogels. Three-dimensional microstructural of collagen hydrogel was performed under the confocal microscopy. Collagen hydrogels cross-linked at indicated conditions were prepared. Atto 550 NHS ester (Sigma-Aldrich) was conjugated to collagen hydrogels according to manufacture's protocol by incubating at room temperature for overnight. Fluorescence-labeled hydrogels were put into a cover glass-bottom confocal dish, overlaid with PBS, and imaged on a multi-photon and confocal microscope system (TCS-SP5-X AOBS, Leica, Germany). Images were collected from 4 random locations of 3 independent hydrogels cross-linked at desired conditions. The fibrils mesh density and size, and pore

density and size were calculated for each image using ImageJ software (1.47v, National Institutes of Health).

In vivo biocompatibility, biodegradation and vasculogenesis assay of the hydrogels

BALB/cAnN.Cg-Foxnlnu/CrlNarl nude mice supplied by National Laboratory Animal Center, Taiwan were used at 6–8 weeks of age. All the protocols were carried out according to the recommendations of the National Tsing-Hua University manual entitled 'Guide for the Care and Use of Laboratory Animals'. Vasculogenesis was evaluated *in vivo* using our xenograft model as described previously [26, 28, 30, 31]. To demonstrate the *in situ* formation of gels *in vivo* and to test for the presence of host immune reactions towards the gels, 200 μL of a mixed solution of collagen-Ph, HRP and H_2O_2 or collagen hydrogels without or with cells (ECFCs and MSCs (2×10^6 total; 40:60= ECFCs: MSCs) was subcutaneously injected into mice before gelation, using a 26-gauge needle, under anesthesia with pentobarbital.

Histological and immunohistochemical analysis

Seven days after injection, each construct was excised, fixed overnight in 4 % neutral buffered formalin, then embedded in paraffin and sectioned along its broad plane. Two 7 μm sections were taken from near the middle of the construct and stained with haematoxylin and eosin (H&E). Density of murine myeloid (numbers/mm^2), microvessel (vessels/mm^2) and adipocyte (adipocytes/mm^2) were reported as the average number in H&E staining slides using ImageJ 1.47v software [26]. The entire area of each section was analyzed. For immunohistochemistry, after deparaffinization and heat antigen retrieval, the sections were cooled down to room temperature and incubated with human-specific CD31 (DakoCytomation) and veimentin (abcam) antibodies. Then, the slides were incubated with biotinylated secondary antibody using an HRP detection system.

Statistical analysis

Three independent experiments were performed for each experimental condition with 3–5 replicates per experiment (n = 3–5) and results are presented as the mean ± standard deviation. Differences between the values were assessed one-way/two-way ANOVA. P-values less than 0.1, 0.01, 0.001 were considered statistically significant and were labeled *, ** *and* ***.

3. Results and Discussion

The gelation mechanism of hydrogel formation can be categorized into either physical crosslinking (physical gelation) or chemical crosslinking (chemical gelation), resulting in different properties: Physically crosslinked collagen hydrogels can be produced after neutralization of the acid solution and subsequent heating to body temperature, i.e. self-assembly of collagen hydrogels (collagen hydrogel, Figure 1a); Chemically crosslinked collagen hydrogels can be achieved through the reaction of their -COOH carboxyl groups with phenolic group (Ph), cross-linkers catalyzed by hydrogen peroxide (H_2O_2) and horseradish peroxidase (HRP), i.e. enzyme-catalyzed collagen-Ph hydrogels (collagen-Ph hydrogel, Figure 1b). The primary difference between these two-collagen hydrogel materials

is the nature of their cross-linking bonds, which also results in diffusion, microstructure and mechanical differences, the covalently cross-linked collagen-Ph hydrogel being less permeable, dense and stronger network under the same mechanical properties G' (Figure 1c-d). Our extracted collagen molecules were used as the starting materials to ensure equal bioactivity of the two cross-linked collagen hydrogels. Next, physicochemical properties of the physically (collagen) and chemically (collagen-Ph) cross-linked hydrogels were determined after polymerization. Finally, the relationships among microstructure, concentration, mechanical properties of the collagen hydrogels, and three-dimensional engineered vascular network were investigated.

3.1. Physically cross-linked collagen hydrogels have limited tunable physicochemical properties

Native collagen molecules are able to self-assemble into collagen fibrils and form hydrogels through physical crosslinking at 37°C and near neutral pH *in vitro*. The physicochemical properties of collagen hydrogels are influenced by collagen concentration, polymerization pH, and ionic strength during crosslinking [32, 33, 34]. Because altering the polymerization pH and ionic strength would be harmful to the cells encapsulated inside hydrogels, collagen concentration seems to be the only suitable parameter to alter the physicochemical properties of collagen hydrogels [18, 23]. Here, pH 7.4 and 37 °C were selected as cross-linking conditions to form collagen hydrogels, and the characterization of material properties was performed as follows. With increasing concentration of collagen molecules, the gelation time of the collagen hydrogel decreased from 739±9 to 186±3 s while its storage modulus (G') similarly increased from 22.13 ± 2.11 to 229.32±5.88 Pa, and the gels turned more opaque (Figure 2a). Results show that the gelation time and storage modulus of collagen hydrogels are somewhat tunable and are highly dependent on the concentration of collagen molecules. The swelling ratio dramatically decreased from 170 to 50 % with increasing concentrations between 0.15 and 0.6 % (Figure 2b), while the diffusion distances always remained constant at ~4 mm (Figure 2c). The microstructure of collagen hydrogels was investigated by confocal microscopy showing that varying the collagen concentration significantly altered the density and diameter of local 3D fibrils (Figure 2d-f). Mesh volume fraction (mesh density, MD) calculated from confocal microscopy images increased linearly with increasing collagen concentration (C) and could be described by the following equation MD=31159.7C-1283.26 *(R^2=0.945)*. The average mesh size (MS) increased slightly and linearly with increasing collagen concentration by the equation MS=1062.3C-343.7 *(R^2=1)*. Mechanical testing of the collagen hydrogels in oscillatory shear showed that G' was positively correlated with the collagen concentration and mesh density. G' varied as a function of collagen concentration and is described by the equation G' = 453.7C-46.97 (*R^2 = 0.996*). The Pearson correlation coefficient was utilized to quantify the relationships among physicochemical properties of collagen hydrogel, namely G', concentration of collagen molecules (arginine-glycine-aspartic acid (RGD) and matrix metalloproteinases (MMP)), swelling, diffusion, mesh size, and mesh density (Table 1a). The concentration of the collagen hydrogel was highly and positively correlated with G', mesh size, and density ($|r|$ <0.7), but negatively correlated with swelling and diffusion (0.40 <$|r|$<0.69). Varying the collagen concentration of physically cross-linked collagen hydrogels also alters gel stiffness, swelling, diffusion, mesh size, and density simultaneously, so it is difficult to decouple the

effects of stiffness and mesh structure from collagen concentrations on three-dimensional vascular network formation using this physically cross-linked collagen hydrogel system.

3.2. Chemically cross-linked collagen-Ph hydrogels have highly tunable physicochemical properties

The advantage of chemical cross-linking of hydrogels, i.e. photo- or enzyme-catalyzed, is the capability to adjust G' and gelation time independently with protein concentration[13, 15, 17, 26, 35]. Here, using modified methods we successfully synthesize chemically cross-linked collagen (collagen-Ph) hydrogels with higher tunable physicochemical properties and lowest hemolysis (data not shown) as compared with previous study[26]. Figure 3a shows that gelation time was tunable by altering HRP concentration at fixed H_2O_2 or by altering H_2O_2 concentration with a fixed concentration of HRP. These results indicate that collagen-Ph hydrogels can form within dozens of seconds, or within several minutes, by simply controlling the concentrations of HRP and H_2O_2. From macroscopic images (data not shown), there was no difference in the opacity of hydrogels with increasing protein concentration, H_2O_2 concentration via HRP-catalysis, and synthesized pH values. Figure 3b demonstrates that the rheological properties (G') of collagen-Ph hydrogels were tunable, ranging from 31.0 ± 0.3 Pa to 623.9 Pa by modifying the amounts of HRP, H_2O_2, and collagen-Ph conjugates. Additionally, the freeze-dried collagen-Ph conjugates are easy to transport and can be stored at room temperature.

To investigate the effects of microstructure, stiffness, and concentration of collagen hydrogels independently on vascular network formation, collagen-Ph hydrogels with the same concentrations (0.15, 0.3, and 0.6 %) and storage moduli (i.e. 50, 100 and 200 Pa) as the collagen hydrogel were synthesized using suitable concentrations of HRP and H_2O_2. All subsequent studies were performed with these particular formulations of collagen-Ph hydrogels unless noted otherwise.

Collagen-Ph hydrogels possessed similar swelling properties, ranging from 154.21±50.41 to 72.86±21.95 % (Figure 3c), regardless of what collagen concentration and G' we used. Except for the 0.15 % collagen-Ph hydrogel with G' of 50 and 100 Pa, all others possessed a significantly lower diffusion distance (<2 mm, Figure 3d) compared with the collagen hydrogels (>4 mm, Figure 2c). The microstructure of collagen-Ph hydrogels indicated a submicro-porous nature when investigated by confocal microscopy (Figure 4). With increasing G' at a constant concentration, the pore density increased and the pore size remained the same, with barely any pores seen in all 0.6 % collagen-Ph hydrogels. On the other hand, with increasing concentration at a constant G', the pore size significantly decreased until becoming non-detectable (Figure 4b-c). Taken together, the honeycomb-like microstructures of collagen-Ph hydrogels can be adjusted independently and individually by either G' or collagen concentration. The Pearson correlation coefficient was utilized to quantify the relationship among physicochemical properties of the collagen-Ph hydrogel (Table 1b). The concentration of the collagen-Ph hydrogel was not related to G' ($r = 0$), had a low strength of correlation with swelling and microstructures ($|r| < 0.39$), and was highly negatively correlated with diffusion distance ($|r| > 0.7$).

Using the above two collagen hydrogel systems allowed for the independent and individual investigation of the effects of cross-linked microstructure, stiffness, and concentration of collagen hydrogels on vascular network formation as follows: First, by using different crosslinking mechanisms, the effects of hydrogel microstructure can be isolated while stiffness and concentration were held constant. Then, the effects of stiffness and collagen concentration on vascular network formation could be clarified by using collagen-Ph hydrogels due to the fact that the concentration of the collagen-Ph hydrogels was not related to stiffness (Table 1).

3.3 Cross-linking modulation of neovascularization

To determine whether controlling crosslinking methods of collagen hydrogel could manipulate the formation of vascular networks *in vivo*, the cell-laden construct formed by adding human ECFCs and MSCs to a collagen pre-polymer solution was injected subcutaneously into mice. Vascular network formation in collagen cell-laden constructs was affected by collagen concentration, as the number of perfused blood vessels inside the construct decreased with increasing collagen concentrations (0.15 %: 213 ± 29 lumens/mm^2; 0.6 %: 112 ± 19 lumens/mm^2, Figure 5,6a). There was no difference in the newly formed lumen area in all collagen cell-laden hydrogels (Figure 6b). Nearly 66 % of newly formed microvessels, identified by staining for hCD31+ (Figure 7), were human microvessels seen within the 0.15 % collagen cell-laden hydrogels; this was followed by an increase to 100 % in 0.3 and 0.6 % collagen cell-laden hydrogels. Additionally, there was an increase in the weight of the engineered tissue construct observed with higher concentration of collagen cell-laden hydrogels (Figure 6c).

To determine whether the different cross-linked bonds could control the formation of vascular networks *in vivo*, collagen-Ph cell-laden constructs with desired collagen concentration and G' (0.15%: 50 Pa; 0.3 %: 100 Pa; 0.6%: 200 Pa) were formed using the appropriate concentrations of HRP and H_2O_2. H&E staining revealed less formation of vascular networks in chemically cross-linked collagen-Ph hydrogels compared with physically cross-linked collagen hydrogels at the same concentration and stiffness, while the lumen area and weight of engineered tissue constructs showed no difference. Results showed that different cross-linking methods did play an important role in the numbers of microvessels formed, and in particular the self-assembled collagen hydrogels enhance and support ECFC/MSCs to form engineered mature microvessels anastomosed with host blood vessels.

To determine whether stiffness could control the formation of vascular networks *in vivo*, we implanted cell-laden collagen-Ph hydrogels at the same concentration and pore size but with different stiffness into immunodeficient mice. Histological results show that a G' of 100 Pa seems to be the most suitable condition compared to the other hydrogels with G' of 50 Pa and 200 Pa. There is no significant difference in the newly formed lumen area and weight of engineered tissue constructs. The percentage of human microvessels (hCD31+) significantly decreased with increasing stiffness at the same concentration, but the percentage is still above 80 % within 0.15 to 0.6% collagen-Ph hydrogels with a G' of 50 and 100 Pa.

To determine whether the collagen concentration could enhance the formation of vascular networks *in vivo*, we implanted cell-laden collagen-Ph hydrogels at the same stiffness and pore size but with different collagen concentrations into immunodeficient mice. Results show that increasing collagen-Ph concentrations from 0.15 to 0.6 % with the same G' decreased the number of lumens inside the construct and resulted in an increase of the weight of the engineered tissue constructs. Additionally, the weight of engineered tissue constructs was highly related to collagen concentration in both collagen hydrogels and collagen-Ph hydrogels. This implies that the concentrations of collagen (i.e. MMP and RGD) did not support vascular formation in chemically cross-linked collagen hydrogels but did influence the dimensions of the engineered construct.

2.4. Interaction between collagen hydrogel and host cells

We previously demonstrated that the recruitment of host myeloid cells is a necessary step in ECFC/MSC-mediated neovascularization [13, 16, 36]. Here, we examined whether the differences observed in micro-vascular density between constructs with various cross-linking methods, stiffness, and collagen concentrations were associated with variations in the recruitment of host cells (Figure 8). To this objective, we examined constructs from both collagen hydrogel systems after 7 days *in vivo* for biodegradation and histological analysis. Our results revealed tunable biodegradation, as demonstrated by changes in the weight percentage (Figure 8a) of explanted hydrogels with different crosslinking degrees and methods. H&E staining of the explanted samples revealed that biodegradation of collagen hydrogels enabled the ingrowth of predominantly non-inflammatory cells to different degrees and the almost complete replacement of the hydrogel with autologous tissue. These results confirmed that collagen hydrogels could be efficiently biodegraded *in vivo*, through the enzymatic hydrolysis of the collagen scaffold. The degradation was quantified by measuring the loss of weight (Figure 8a). Both 0.15 and 0.3 % collagen hydrogels degrade more than 95 % after 7 days, but increasing the concentration to 0.6 % slows degradation to 90 %. Regardless of G', the same trend was observed in collagen-Ph hydrogels, i.e. all 0.15 and 0.3 % collagen-Ph hydrogels degrade more than 95 %, and increasing the concentration to 0.6 % collagen-Ph also slowed down the degradation to ~90%. As expected, the commercial control collagen gel degraded rapidly, at 96.89 %, which is almost the same degradation rate as our extracted 0.3 % collagen hydrogels (96.68%). Results show that the degradation is highly correlated with collagen concentration instead of crosslinking methods in both collagen hydrogel systems.

H&E staining was also analyzed by calculating the number of leukocytes accumulated in the boundaries between the hydrogel and the host tissue (Figure 8b) and infiltrated inside hydrogels (Figure 8c). H&E images revealed no significant difference in the number of leukocytes accumulated at the boundaries of both collagen and collagen-Ph hydrogels in all crosslinking conditions. In contrast, more leukocyte infiltration was observed in collagen hydrogels than collagen-Ph hydrogels with the same concentration of collagen. With increasing concentration of collagen hydrogels, less leukocyte infiltration was observed, and the same trend was observed in collagen-Ph hydrogels with increasing concentration at the same stiffness. The rate of biodegradation for collagen hydrogels *in vivo* was shown to be modulated by variations in the concentrations of the collagen but not correlated with

microstructure and crosslinking methods. However, the microstructure of hydrogels could influence the number of infiltrating leukocytes. Therefore, it is possible to finely tune the amount of time that the hydrogels remain associated with tissues to ensure proper mechanical support and also to control the number of infiltrating host leukocytes to elicit a complex physiological repair and regenerative response.

3.5 Correlation between physicochemical material properties, the extent of material-mediated host immune response and engineered vascularized constructs

In order to demonstrate how and why physicochemical properties of collagen hydrogels regulate the extent of the ECFC-MSC based vascular network formation, the perfused functional lumen density and size, weight of engineered vascularized constructs, and percentage of human cells (hCD31+) within the lumen were plotted against the hydrogel properties (G', concentration of RGD and MMP, swelling, diffusion, mesh size, mesh density, and *in vivo* bio-degradation) and host immune response (murine leukocytes surrounding and inside the hydrogel constructs) of the self-assembled collagen hydrogels (Table 2a), enzymatically cross-linked collagen-Ph hydrogels (Table 2b), and collagen hydrogels (i.e. no matter which crosslinking methods used, Table 2c). Correlation was assessed using linear regression and the *r* (correlation coefficient) value. In physically cross-linked collagen hydrogels, the lumen density is proportional to the diffusion rate (*r =1***) and number of murine leukocytes inside gels (*r=0.89***, Table 2a). These results revealed that the extent of vascular network formation is highly dependent on the diffusion of gels and the number of infiltrating host leukocytes observed inside gels. High concentration collagen gels were stiffer with less swelling and diffusion properties, higher mesh density and diameter, and resulted in less infiltrating murine leukocytes, showing that these constructs have less microvessel density and smaller lumens. These observations are in line with recent reports [15, 17, 18, 21, 29] that correlate ECM mechanical properties and capillary cell shape and function. On the other hand, in collagen-Ph hydrogels (Table 2b), diffusion (*r=0.46***), *in vivo* degradation (*r=0.50***), and the number of murine leukocytes inside gels (*r=0.57***) also play an important role in lumen formation within the construct. A higher diffusion and biodegradation rate of collagen-Ph hydrogels resulted in more infiltrating murine leukocytes, illustrating that these constructs have higher microvessel density and smaller lumens; these results are in line with our previous studies [26, 29] and recent research [15, 17, 21, 29] that correlate ECM mechanical properties and capillary cell shape and function. Regardless of which cross-linking methods (Table 2c) were used to polymerize collagen, the lumen density inside collagen gels is proportional to the diffusion property of gels (*r=0.75***) and the degree of infiltration by murine leukocytes (*r=0.88***). Moreover, the weight and diameter of engineered collagen tissue constructs are highly proportional to the concentration of collagen instead of the crosslinking methods and stiffness. Taken together, to engineer a large vascularized tissue construct within 7 days, an ideal vascularized hydrogel that can integrate structure with functionality should have several important characteristics, namely, high collagen concentration (RGD/MMP), diffusion properties, and capability to host infiltrating leukocytes, and should be designed to regulate angiogenesis and vasculogenesis.

3.6. Crosslinking modulation of tissue-engineered vascularized adipose tissue constructs in vivo

Next, in order to examine the capability of creating large adipose tissues *in vivo* through simultaneous creation of an intrinsic vascular network with blood supply, collagen and collagen-Ph hydrogels with the same collagen concentration and G' of 50 Pa in the absence of any exogenous cytokines were selected. MSCs and ECFCs were encapsulated into the above indicated collagen hydrogels before gelation, and then injected subcutaneously into nude mice for long-term observation. After one month, the commercial rat-tail collagen gel (type1, Corning, USA) serving as the control was completely degraded with no sign of the implants at the implantation site. Meanwhile, histological examinations of explanted constructs showed less adipose tissue formation (~27.6 adipocytes/mm^2; ~18% area of construct) inside collagen gels (Figure 9), in contrast to the extensive adipose tissue (~877.6 adipocytes/mm^2; 94% area of construct) present inside collagen-Ph constructs (Figure 10). The white adipose tissue observed in both collagen hydrogels was derived from invading host cells rather than implanted cells (h-vimentin-negative), while some hCD31+ ECFC-lined blood vessels (Figure 9c, black arrows) were only observed in collagen-Ph hydrogels. Adipocyte density in cell-laden collagen-Ph constructs was significantly higher than in collagen constructs and even higher than native white adipose tissue (~600 adipocytes/mm^2). The size of adipocytes in cell-laden collagen-Ph constructs is similar to native adipocytes. Additionally, the weight of this engineered white adipose tissue construct using cell-laden collagen-Ph hydrogels was ~25 mg, which is equal to 5 % (w/v) of the mass of whole white fat pads in a mouse. Taken together, we successfully engineered a white adipose tissue construct *in vivo* by controlling the cross-linked methods of collagen hydrogels embedded with ECFCs and MSCs. These results indicate that the polymerized mechanism of the collagen hydrogel could be used to modulate not only the extent of hCD31+ ECFC-lined vascular network formation, but also the regenerative capacity of white adipose tissue in cell-laden constructs *in vivo*.

3. Conclusion

In this study, we developed an injectable cell-laden collagen hydrogel platform for creating live adipose tissue through manipulating vasculogenesis and angiogenesis. By varying polymerization, we fabricated collagen hydrogels with independently tunable microstructure, concentration, and stiffness, and the individual and combined effects of these properties on the short-term extent of vascular network formation were demonstrated. With such a prevascularized tissue approach, results also suggested the polymerized microstructure of cell-laden collagen hydrogels provides a functionalized niche to modulate the long-term regenerative capacity of adipose tissue in such cell-laden constructs *in vivo*. This study emphasizes the importance of the ECM in providing the appropriate architecture for recruitment of host myeloid cells to improve ECFC/MSC-mediated vascular formation, which is critical for the earliest and necessary step of adipogenesis to engineer large-size adipose tissues.

5. Acknowledgements

This work was supported by the Ministry of Science and Technology of Taiwan grant (MOST 105–2221-E-007–142 and MOST 106–2221-E-007–055 to Y.-C. C.) and a National Institutes of Health Grant (R00EB009096, to J.M.M.-M.). The authors acknowledge the National Laboratory Animal Center (funded by the Ministry of Science and Technology of Taiwan) for technical support in the histology-related experiments. Also, the authors also acknowledge assistance from the core facility of Multiphoton and Confocal Microscope System in College of Biological science and Technology, National Chiao-Tung University, Hsinchu, Taiwan.

Reference

1. Van Nieuwenhove I, Tytgat L, Ryx M, et al. Soft tissue fillers for adipose tissue regeneration: From hydrogel development toward clinical applications [Review]. Acta Biomater. 2017 11;63:37–49. doi: 10.1016/j.actbio.2017.09.026. PubMed PMID: ; English. [PubMed: 28941654]
2. Choi JH, Gimble JM, Lee K, et al. Adipose Tissue Engineering for Soft Tissue Regeneration [Article]. Tissue Eng Part B-Rev. 2010 8;16(4):413–426. doi: 10.1089/ten.teb.2009.0544. PubMed PMID: ; English. [PubMed: 20166810]
3. Coleman SR, Saboeiro AP. Fat grafting to the breast revisited: Safety and efficacy [Article; Proceedings Paper]. Plast Reconstr Surg. 2007 3;119(3):775–785. doi: 10.1097/01.prs.0000252001.59162.c9. PubMed PMID: ; English. [PubMed: 17312477]
4. Smith P, Adams WP, Lipschitz AH, et al. Autologous human fat grafting: Effect of harvesting and preparation techniques on adipocyte graft survival [Article; Proceedings Paper]. Plast Reconstr Surg. 2006 5;117(6):1836–1844. doi: 10.1097/01.prs.0000218825.77014.78. PubMed PMID: ; English. [PubMed: 16651956]
5. Rossi E, Gerges I, Tocchio A, et al. Biologically and mechanically driven design of an RGD-mimetic macroporous foam for adipose tissue engineering applications [Article]. Biomaterials. 2016 10;104:65–77. doi: 10.1016/j.biomaterials.2016.07.004. PubMed PMID: ; English. [PubMed: 27428768]
6. Moya ML, Lucas S, Francis-Sedlak M, et al. Sustained delivery of FGF-1 increases vascular density in comparison to bolus administration [Article]. Microvasc Res. 2009 9;78(2):142–147. doi: 10.1016/j.mvr.2009.06.006. PubMed PMID: ; English. [PubMed: 19555698]
7. Liu Z, Kobayashi K, van Dinther M, et al. VEGF and inhibitors of TGF beta type-I receptor kinase synergistically promote blood-vessel formation by inducing alpha 5-integrin expression [Article]. J Cell Sci. 2009 9;122(18):3294–3302. doi: 10.1242/jcs.048942. PubMed PMID: ; English. [PubMed: 19706683]
8. Matsui M, Tabata Y. Enhanced angiogenesis by multiple release of platelet-rich plasma contents and basic fibroblast growth factor from gelatin hydrogels [Article]. Acta Biomater. 2012 5;8(5):1792–1801. doi: 10.1016/j.actbio.2012.01.016. PubMed PMID: ; English. [PubMed: 22293581]
9. Jain RK, Au P, Tam J, et al. Engineering vascularized tissue [Editorial Material]. Nat Biotechnol. 2005 7;23(7):821–823. doi: 10.1038/nbt0705-821. PubMed PMID: ; English. [PubMed: 16003365]
10. Baiguera S, Ribatti D. Endothelialization approaches for viable engineered tissues [Review]. Angiogenesis. 2013 1;16(1):1–14. doi: 10.1007/s10456-012-9307-8. PubMed PMID: ; English. [PubMed: 23010872]
11. Tian L, George SC. Biomaterials to Prevascularize Engineered Tissues [Article]. J Cardiovasc Transl Res. 2011 10;4(5):685–698. doi: 10.1007/s12265-011-9301-3. PubMed PMID: ; English. [PubMed: 21892744]
12. Lovett M, Lee K, Edwards A, et al. Vascularization Strategies for Tissue Engineering [Review]. Tissue Eng Part B-Rev. 2009 9;15(3):353–370. doi: 10.1089/ten.teb.2009.0085. PubMed PMID: ; English. [PubMed: 19496677]
13. Lin RZ, Moreno-Luna R, Li D, et al. Human endothelial colony-forming cells serve as trophic mediators for mesenchymal stem cell engraftment via paracrine signaling [Article]. Proc Natl Acad Sci U S A. 2014 7;111(28):10137–10142. doi: 10.1073/pnas.1405388111. PubMed PMID: ; English. [PubMed: 24982174]

14. Melero-Martin JM, Khan ZA, Picard A, et al. In vivo vasculogenic potential of human blood-derived endothelial progenitor cells [Article]. Blood. 2007 6;109(11):4761–4768. doi: 10.1182/blood-2006-12-062471. PubMed PMID: ; English. [PubMed: 17327403]
15. Chen YC, Lin RZ, Qi H, et al. Functional Human Vascular Network Generated in Photocrosslinkable Gelatin Methacrylate Hydrogels [Article]. Adv Funct Mater. 2012 5;22(10):2027–2039. doi: 10.1002/adfm.201101662. PubMed PMID: ; English. [PubMed: 22907987]
16. Lin RZ, Lee CN, Moreno-Luna R, et al. Host non-inflammatory neutrophils mediate the engraftment of bioengineered vascular networks [Article]. Nat Biomed Eng. 2017 6;1(6):12. doi: 10.1038/s41551-017-0081. PubMed PMID: ; English.
17. Lin RZ, Chen YC, Moreno-Luna R, et al. Transdermal regulation of vascular network bioengineering using a photopolymerizable methacrylated gelatin hydrogel [Article]. Biomaterials. 2013 9;34(28):6785–6796. doi: 10.1016/j.biomaterials.2013.05.060. PubMed PMID: ; English. [PubMed: 23773819]
18. Critser PJ, Kreger ST, Voytik-Harbin SL, et al. Collagen matrix physical properties modulate endothelial colony forming cell-derived vessels in vivo [Article]. Microvasc Res. 2010 7;80(1):23–30. doi: 10.1016/j.mvr.2010.03.001. PubMed PMID: ; English. [PubMed: 20219180]
19. Cross VL, Zheng Y, Choi NW, et al. Dense type I collagen matrices that support cellular remodeling and microfabrication for studies of tumor angiogenesis and vasculogenesis in vitro [Article]. Biomaterials. 2010 11;31(33):8596–8607. doi: 10.1016/j.biomaterials.2010.07.072. PubMed PMID: ; English. [PubMed: 20727585]
20. Rao RR, Peterson AW, Ceccarelli J, et al. Matrix composition regulates three-dimensional network formation by endothelial cells and mesenchymal stem cells in collagen/fibrin materials [Article]. Angiogenesis. 2012 6;15(2):253–264. doi: 10.1007/s10456-012-9257-1. PubMed PMID: ; English. [PubMed: 22382584]
21. Mason BN, Starchenko A, Williams RM, et al. Tuning three-dimensional collagen matrix stiffness independently of collagen concentration modulates endothelial cell behavior [Article]. Acta Biomater. 2013 1;9(1):4635–4644. doi: 10.1016/j.actbio.2012.08.007. PubMed PMID: ; English. [PubMed: 22902816]
22. Helary C, Bataille I, Abed A, et al. Concentrated collagen hydrogels as dermal substitutes [Article]. Biomaterials. 2010 1;31(3):481–490. doi: 10.1016/j.biomaterials.2009.09.073. PubMed PMID: ; English. [PubMed: 19811818]
23. McCoy MG, Seo BR, Choi SY, et al. Collagen I hydrogel microstructure and composition conjointly regulate vascular network formation [Article]. Acta Biomater. 2016 10;44:200–208. doi: 10.1016/j.actbio.2016.08.028. PubMed PMID: ; English. [PubMed: 27545811]
24. Mauney JR, Nguyen T, Gillen K, et al. Engineering adipose-like tissue in vitro and in vivo utilizing human bone marrow and adipose-derived mesenchymal stem cells with silk fibroin 3D scaffolds [Article]. Biomaterials. 2007 12;28(35):5280–5290. doi: 10.1016/j.biomaterials.2007.08.017. PubMed PMID: ; English. [PubMed: 17765303]
25. Lee CH, Singla A, Lee Y. Biomedical applications of collagen [Review]. Int J Pharm. 2001 6;221(1–2):1–22. doi: 10.1016/s0378-5173(01)00691-3. PubMed PMID: ; English. [PubMed: 11397563]
26. Kuo KC, Lin RZ, Tien HW, et al. Bioengineering vascularized tissue constructs using an injectable cell-laden enzymatically crosslinked collagen hydrogel derived from dermal extracellular matrix [Article]. Acta Biomater. 2015 11;27:151–166. doi: 10.1016/j.actbio.2015.09.002. PubMed PMID: ; English. [PubMed: 26348142]
27. Lin RZ, Moreno-Luna R, Zhou B, et al. Equal modulation of endothelial cell function by four distinct tissue-specific mesenchymal stem cells [Research Support, N.I.H., Extramural Research Support, Non-U.S. Gov't]. Angiogenesis. 2012 9;15(3):443–55. doi: 10.1007/s10456-012-9272-2. PubMed PMID: ; PubMed Central PMCID: PMC3409933. eng. [PubMed: 22527199]
28. Lin RZ, Melero-Martin JM. Bioengineering human microvascular networks in immunodeficient mice [Research Support, N.I.H., Extramural Video-Audio Media]. J Vis Exp. 2011 (53):e3065. doi: 10.3791/3065. PubMed PMID: ; PubMed Central PMCID: PMC3196173. eng. [PubMed: 21775960]
29. Chuang C-H, Lin R-Z, Tien H- W, et al. Enzymatic regulation of functional vascular networks using gelatin hydrogels. Acta Biomater. 2015. doi: 10.1016/j.actbio.2015.02.024.

30. Melero-Martin JM, De Obaldia ME, Kang SY, et al. Engineering robust and functional vascular networks in vivo with human adult and cord blood-derived progenitor cells [Article]. CircRes. 2008 7;103(2):194–202. doi: 10.1161/circresaha.108.178590. PubMed PMID: ; English.

31. Lin RZ, Melero-Martin JM. Fibroblast growth factor-2 facilitates rapid anastomosis formation between bioengineered human vascular networks and living vasculature [Article]. Methods. 2012 3;56(3):440–451. doi: 10.1016/j.ymeth.2012.01.006. PubMed PMID: ; English. [PubMed: 22326880]

32. Oechsle AM, Landenberger M, Gibis M, et al. Modulation of collagen by addition of Hofmeister salts [Article]. Int J Biol Macromol. 2015 8;79:518–526. doi: 10.1016/j.ijbiomac.2015.05.023. PubMed PMID: ; English. [PubMed: 26014138]

33. Oechsle AM, Wittmann X, Gibis M, et al. Collagen entanglement influenced by the addition of acids [Article]. Eur Polym J. 2014 9;58:144–156. doi: 10.1016/j.eurpolymj.2014.06.015. PubMed PMID: ; English.

34. Yan MY, Li BF, Zhao X, et al. Effect of concentration, pH and ionic strength on the kinetic self-assembly of acid-soluble collagen from walleye pollock (Theragra chalcogramma) skin [Article]. Food Hydrocolloids. 2012 10;29(1):199–204. doi: 10.1016/j.foodhyd.2012.02.014. PubMed PMID: ; English.

35. Chuang CH, Lin RZ, Tien HW, et al. Enzymatic regulation of functional vascular networks using gelatin hydrogels [Article]. Acta Biomater. 2015 6;19:85–99. doi: 10.1016/j.actbio.2015.02.024. PubMed PMID: ; English. [PubMed: 25749296]

36. Lin RZ, Lee CN, Moreno-Luna R, et al. Host non-inflammatory neutrophils mediate the engraftment of bioengineered vascular networks. Nat Biomed Eng. 2017;1. doi: 10.1038/s41551-017-0081. PubMed PMID: ; PubMed Central PMCID: PMCPMC5578427. [PubMed: 28868207]

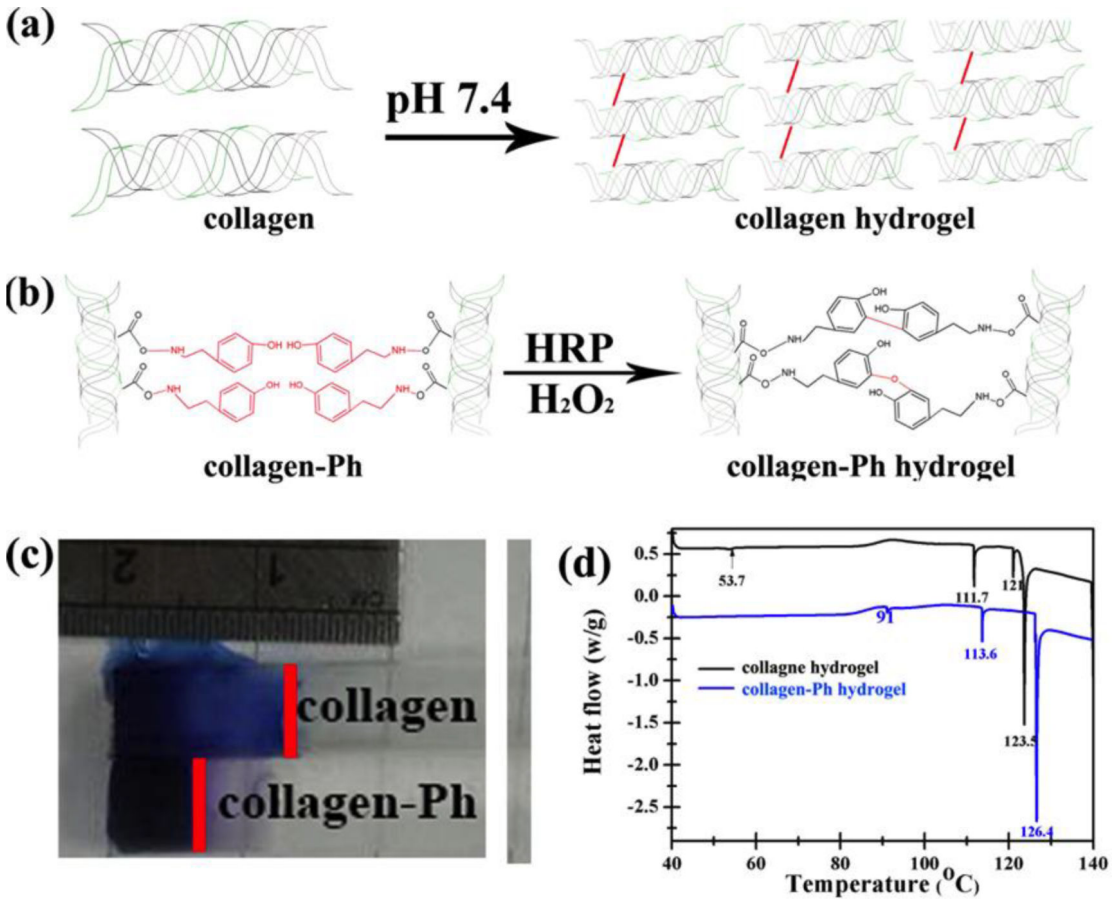

Figure 1.

Formation of (a) physical cross-linked collagen hydrogels and (b) chemical cross-linked collagen-Ph hydrogels. The difference in (c) diffusion property and (d) energy of crosslinking bonds performed by differential scanning calorimetry on collagen and collagen-Ph hydrogels with same collagen concentration of 0.3 % and storage modulus of 100 Pa.

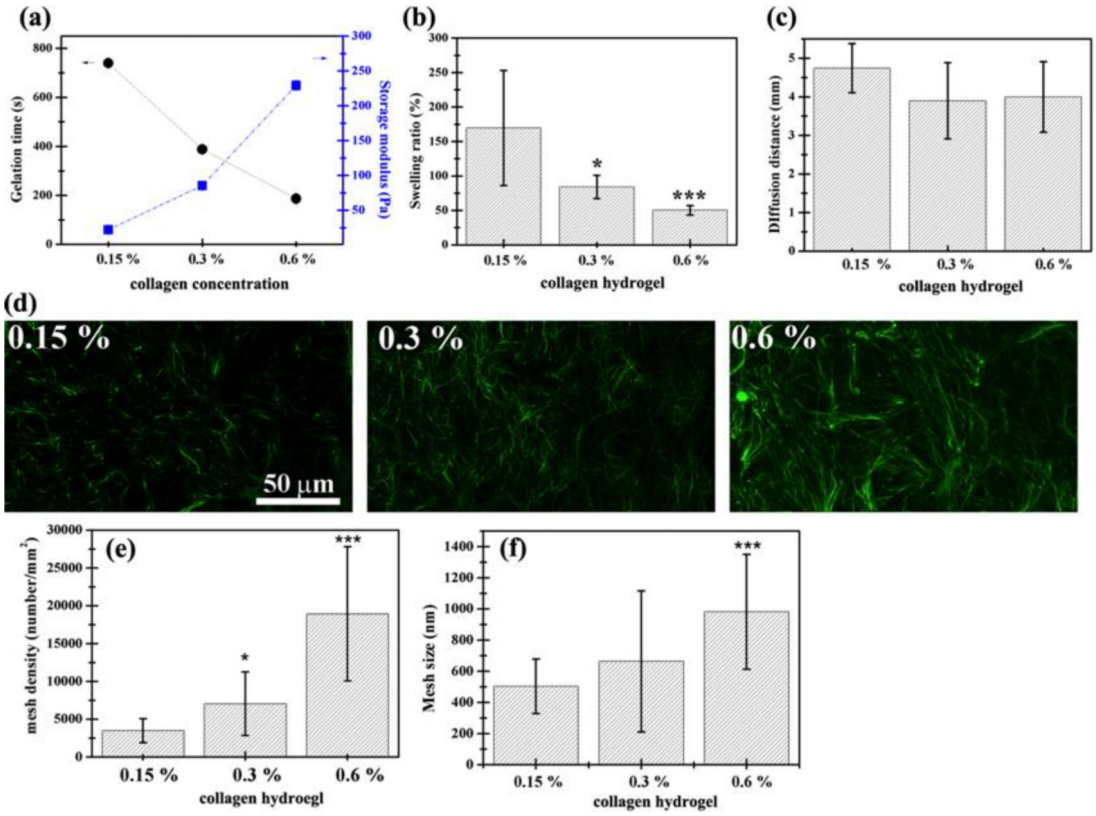

Figure 2.

Physical properties of physical cross-linked collagen hydrogels vary with collagen concentration with limited tunability. (a) Gelation time decreased and shear storage modulus (G') increased with increasing collagen concentration. (b) Swelling properties decreased with increasing collagen concentration. (c) Diffusion properties of 3D collagen hydrogel remains the same with increasing collagen concentration. (d-f) Mesh density increased linearly with collagen concentration as shown in (d) 3D confocal microscopy images. (e-f) Summarized data of 0.15, 0.3, and 0.6 % collagen hydrogels. P-values less than 0.1 and 0.001 were considered statistically significant and were labeled * and *** compared with the 0.15 % collagen hydrogel.

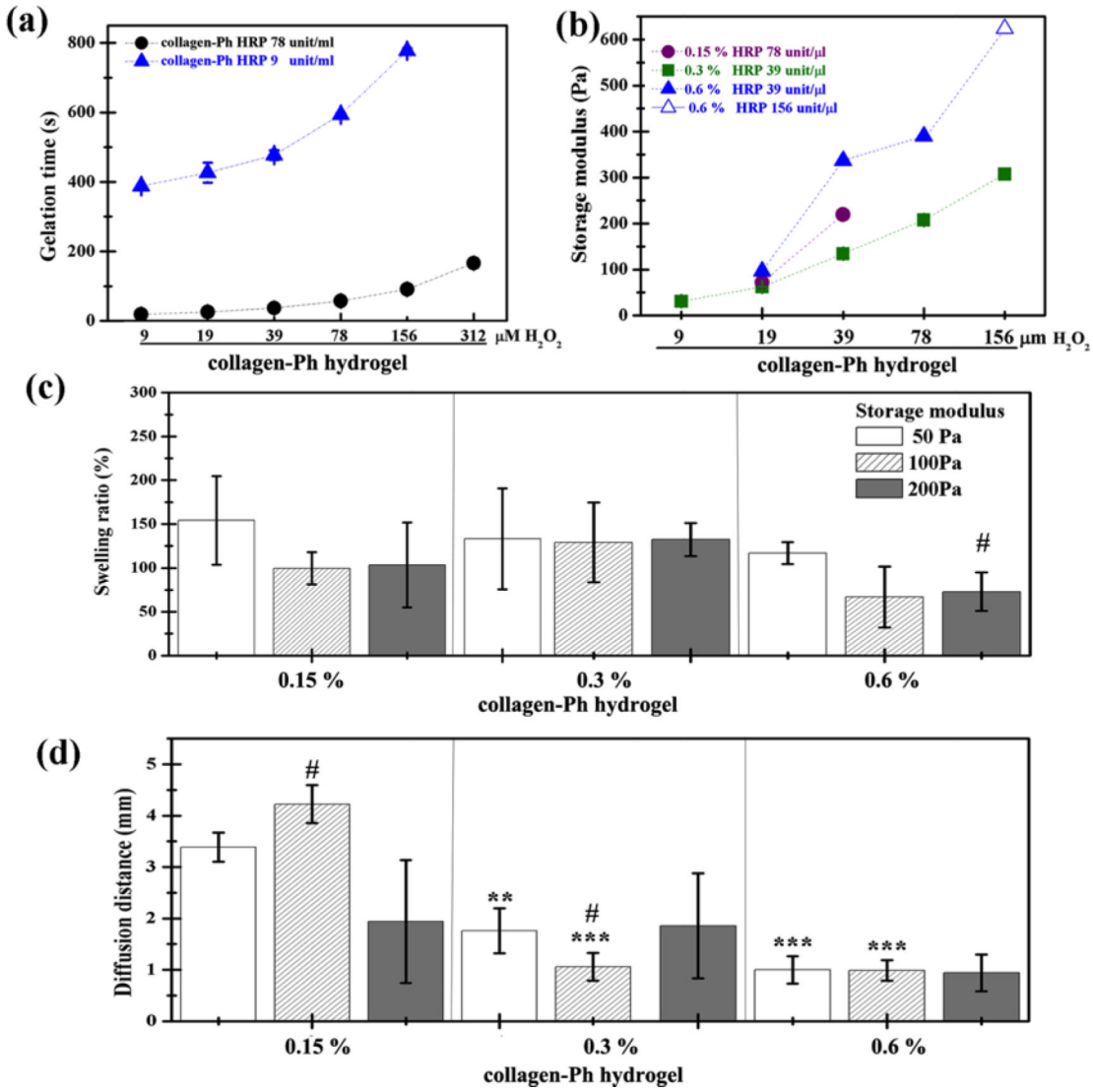

Figure 3.

Tunable physical properties of chemical cross-linked collagen-Ph hydrogels varied with HRP, H_2O_2, and collagen-Ph concentration. (a) Gelation time was adjustable by HRP concentration. (b) Shear storage modulus (G') increased with increasing collagen concentration and H_2O_2 concentration with a suitable amount of HRP. (c) Swelling properties remained constant with increasing collagen-Ph concentration or increasing G'. (d) Diffusion properties of collagen-Ph hydrogel as a function of collagen-Ph concentration and G'. Diffusion distances are larger than 3 mm for 0.15 % collagen-Ph hydrogels with G'=50 and 100 Pa, whereas others are below 2 mm. P-values less than 0.01 and 0.001 were considered statistically significant and were labeled ** and *** compared with the 0.15% collagen-Ph hydrogel with the same G'. P-values less than 0.1 were considered statistically significant and were labeled # compared with the collagen-Ph hydrogel with G' of 50 Pa at the same concentration.

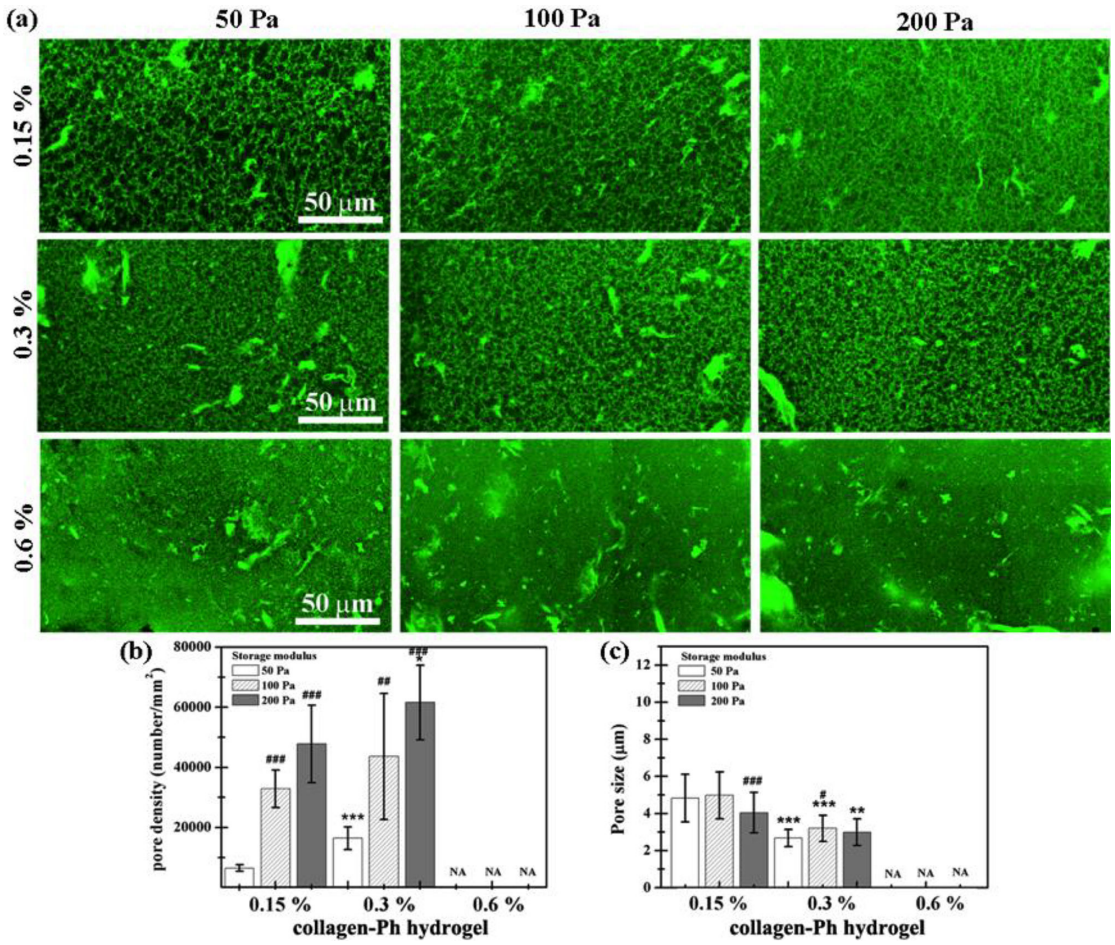

Figure 4.

Collagen-Ph hydrogel microstructure as a function of collagen-Ph concentration and G'. (a) 3D confocal microscopy images and (b-c) summarized data for pore density and pore size are shown. P-values less than 0.01, 0.001 were considered statistically significant and were labeled ** and *** compared with the 0.15 % collagen-Ph hydrogel with the same G'. P-values less than 0.1, 0.01, 0.001 were considered statistically significant and were labeled #, ##, and ###, respectively compared with the collagen-Ph hydrogel with G' of 50 Pa at the same concentration.

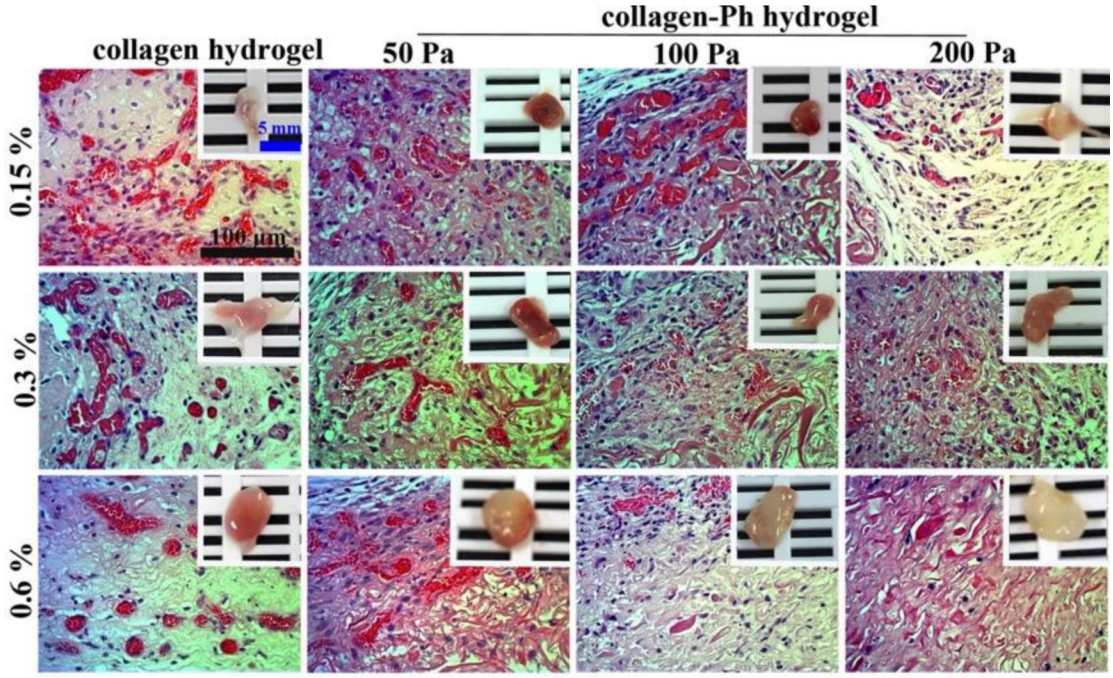

Figure 5.

Crosslinking modulation of vascularized collagen constructs containing human ECFCs and MSCs collagen or collagen-Ph explanted after 7 days *in vivo*. H&E-stained images of vascularized collagen constructs with different cross-linking methods, G', and protein concentrations, showing erythrocyte-filled lumens. The insets in the top panels show macroscopic views of the explants (scale bar 5 mm).

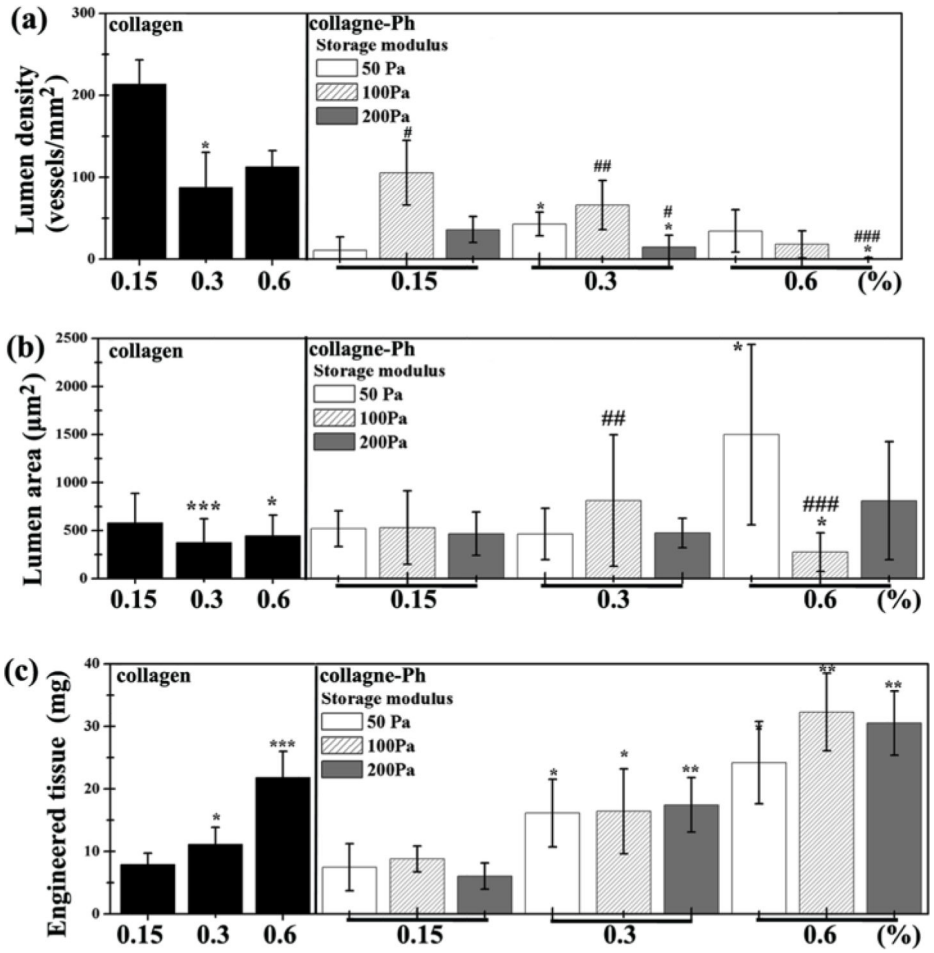

Figure 6.

(a) Lumen density, (b) lumen area, and (c) weight of engineered cell-laden collagen (left) or collagen-Ph (right) tissue constructs were quantified. P-values less than 0.1, 0.01, 0.001 were considered statistically significant and were labeled *, **, and *** compared with the 0.15 % collagen-Ph hydrogel with the same G'. P-values less than 0.1, 0.01, 0.001 were considered statistically significant and were labeled #, ##, *and* ### compared with the collagen-Ph hydrogel with G' of 50 Pa at the same concentration.

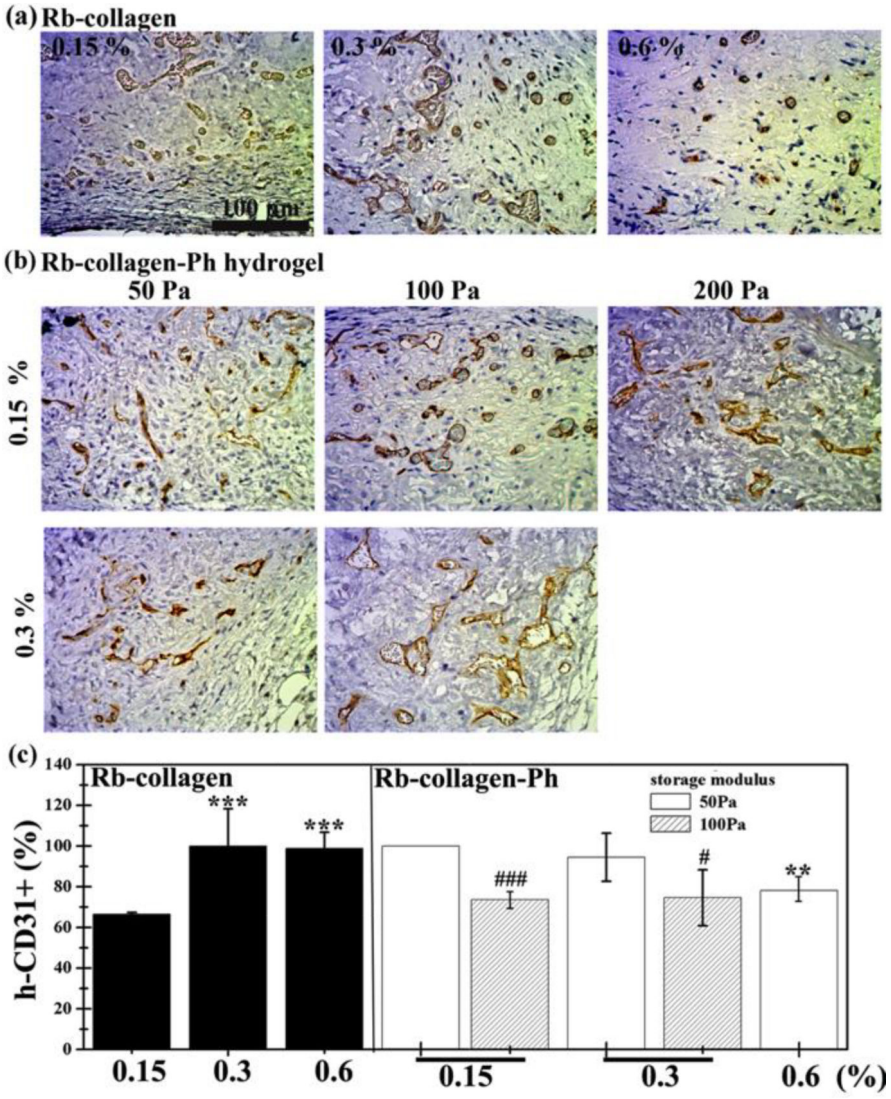

Figure 7.

Crosslinking modulation of human ECFCs-MSC-mediated vascular network formation in collagen (left) or collagen-Ph (right) hydrogels after 7 days *in vivo*. Representative images of sections stained with human CD31+ ECFCs identified by immunohistochemistry shown in (a) collagen and (b) collagen-Ph hydrogels at various conditions. (c) The extent of human vascular network formation was quantified by counting erythrocyte-filled lumens, showing the percentage of the total blood vessels expressing human CD31. In collagen hydrogels, P-values less than 0.001 were considered statistically significant and were labeled *** compared with the 0.15% collagen hydrogel. In collagen-Ph hydrogels, P-values less than 0.01 were considered statistically significant and were labeled ** compared with the 0.15% collagen-Ph hydrogel with the same G'. P-values less than 0.1 and 0.001 were considered statistically significant and were labeled # and ### compared with the collagen-Ph hydrogel with G' of 50 Pa at the same concentration.

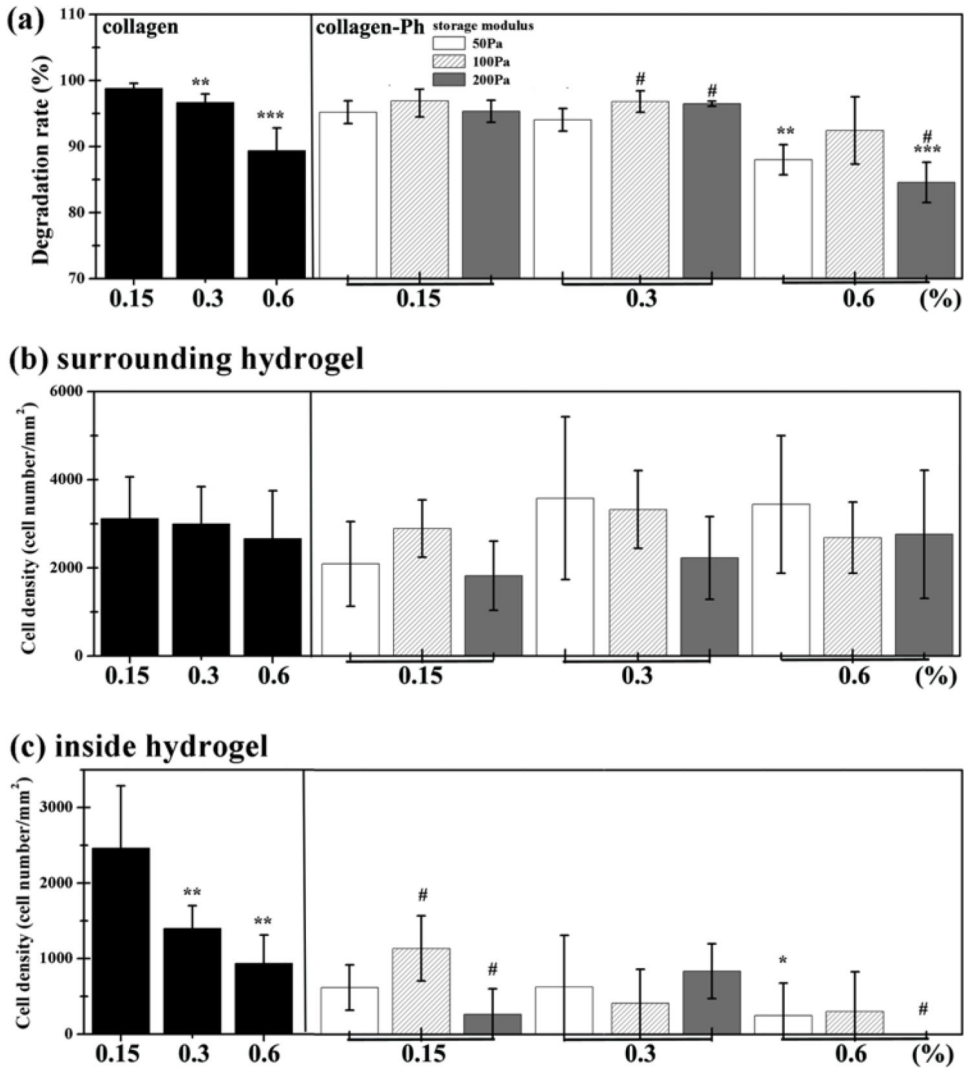

Figure 8.

Crosslinking modulation of biodegradation and host cell recruitment. Collagen and collagen-Ph solutions were subcutaneously injected into nude mice and polymerized to form collagen (left) and collagen-Ph (right) hydrogels. Constructs were evaluated after 7 days *in vivo*. (a) Modulation of *in vivo* degradation profiles on collagen hydrogels and collagen-Ph hydrogels with various amounts of collagen-Ph and G'. Quantification of total murine myeloid cells (b) surrounding host tissue and (c) inside the hydrogel constructs. In collagen hydrogels, P-values less than 0.01 and 0.001 were considered statistically significant and were labeled ## and ### compared with the 0.15% collagen hydrogel. In collagen-Ph hydrogels, P-values less than 0.1, 0.01, 0.001 were considered statistically significant and were labeled *, **, and *** compared with the 0.15% collagen-Ph hydrogel with the same G'. P-values less than 0.1 were considered statistically significant and were labeled # compared with the collagen-Ph hydrogel with G' of 50 Pa at the same concentration.

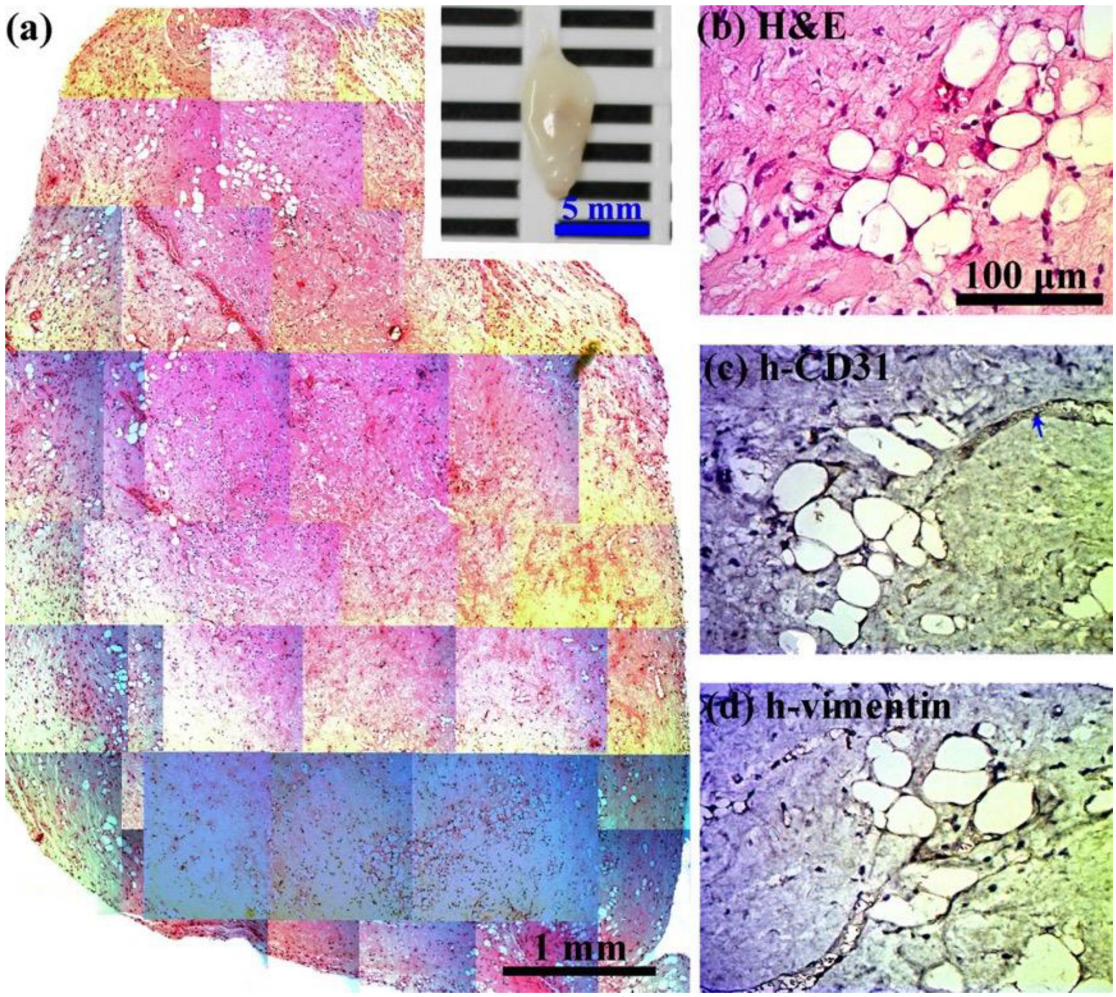

Figure 9.

Crosslinking modulation of vascularized adipose tissue graft in cell-laden collagen hydrogels. 0.6 % Collagen pre-polymer solutions with ECFCs and MSCs in the absence of any exogenous cytokines were subcutaneously injected into nude mice and formed cell-laden collagen hydrogels. Constructs were evaluated after 1 month *in vivo*. (a) The macroscopic view (inset, scale bar 5 mm) and representative H&E-stained section of entire cell-laden collagen constructs are shown (scale bar 1 mm). (b-d) High magnification of selected regions show some murine adipocytes (human-vimentin-negative) with murine vessels (human CD31-negative, blue arrows) carrying erythrocytes.

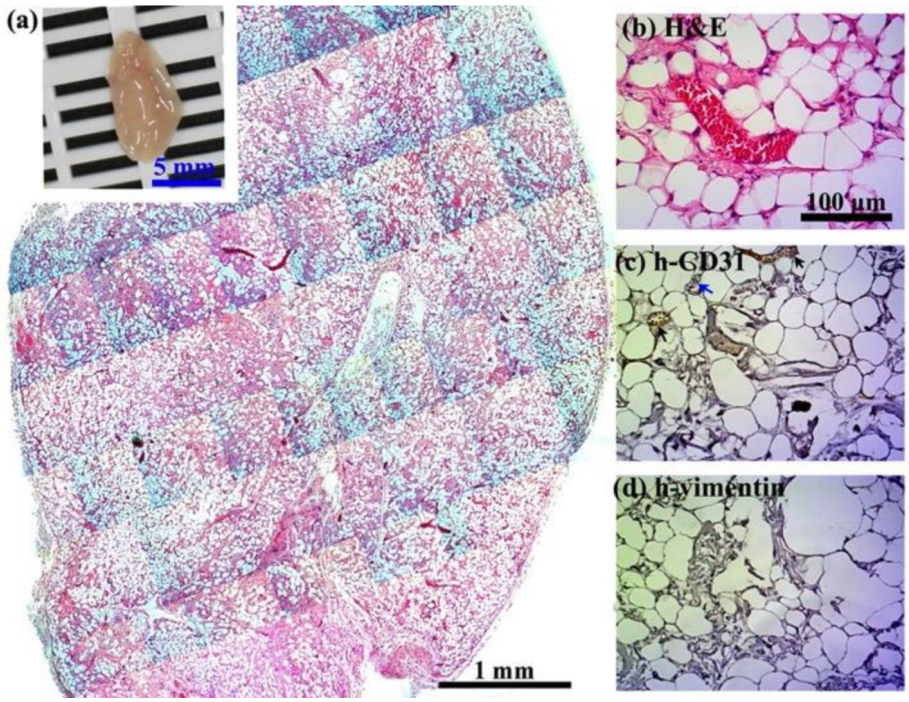

Figure 10.

Crosslinking modulation of vascularized adipose tissue graft in collagen-Ph hydrogels. 0.6% Collagen-Ph pre-polymer solutions with ECFCs and MSCs in the absence of any exogenous cytokines were subcutaneously injected into nude mice and formed cell-laden collagen-Ph hydrogels under suitable concentrations of HRP and H_2O_2. Constructs were evaluated after 1 month *in vivo.* (a) The macroscopic view (inset, scale bar 5 mm) and representative H&E-stained section of entire cell-laden collagen-Ph constructs are shown (scale bar 1 mm). Adipose tissue covers entire construct. (b-d) High magnification of selected regions shows some murine adipocytes (human vimentin-negative) with some human vessels (human CD31-positive, black arrows)/murine vessels (human CD31-negative, blue arrows) carrying erythrocytes.

Table 1.

Pearson coefficients of correlation (r) among various physicochemical properties, i.e. G', concentration of collagen (RGD and MMP), swelling, diffusion, mesh size, and mesh density of the (a) physical crosslinked collagen hydrogel and (b) chemical crosslinked collagen-Ph hydrogel. High correlation (in red): $|r|>0.70$; medium correlation (in blue): $0.40 < |r| < 0.69$; low correlation (in black): $|r| < 0.39$.

(a)Rb-collagen	[RGD], [MMP]	G'	swelling	diffusion	mesh size	mesh density
[RGD], [MMP]	1					
G'	0.98	1				
swelling	−0.69	−0.72	1			
diffusion	−0.68	−0.55	0.93	1		
mesh size	0.99	0.99	−0.91	−0.68	1	
mesh density	0.99	0.99	−0.85	−0.59	0.99	1

(b) Rb-collagen-Ph	[RGD], [MMP]	G'	swelling	diffusion	pore size	pore density
[RGD], [MMP]	1					
G'	0.00	1				
swelling	0.31	−0.22	1			
diffusion	−0.76	−0.23	−0.49	1		
pore size	0.20	−0.69	0.68	−0.30	1	
pore density	0.31	0.88	0.27	−0.43	−0.36	1

Table 2.

Pearson coefficients of correlation (r) among various physicochemical material properties (G', concentration of collagen (RGD and MMP), swelling, diffusion, mesh size, mesh density, and *in vivo* bio-degradation), host immune response (murine myeloid cells surrounding and inside the hydrogel constructs), and properties of engineered vascularized construct (weight of engineered construct, lumen density, lumen size, and percentage of engineered human lumen) of the (a) physical cross-linked collagen hydrogels, (b) chemical cross-linked collagen hydrogels, and (c) collagen hydrogels (i.e. no matter which crosslinking methods used). High correlation (in red): $|r|>0.70$; medium correlation (in blue): $0.40<|r|<0.69$; low correlation (in black): $|r|<0.39$.

(a)Rb-collagen hydrogel		**Enginnered tissue construct**			
		weight	**lumen density**	**lumen area**	**hCD31+**
materials properties	[RGD], [MMP]	0.99	−0.48	−0.44	0.73
	G'	0.98	−0.29	−0.41	0.61
	swelling	−0.60	0.18	0.90	−0.95
	diffusion	−0.60	1.00	0.97	−1.00
	mesh size	0.99	−0.62	−0.49	0.74
	mesh density	1.00	−0.53	−0.38	0.65
	in vivo degradation	−0.98	0.34	0.43	−0.65
immune response	inside hydrogel	−0.80	0.89	0.32	−0.94
	surrounding hydrogel	−0.41	0.63	−0.48	−0.67

(b)Rb-collagen-Ph hydrogel		**Enginnered tissue construct**			
		weight	**lumen density**	**lumen area**	**hCD31+**
materials properties	[RGD], [MMP]	0.98	−0.42	0.45	−0.29
	G'	0.02	−0.30	−0.23	−0.87
	swelling	0.41	0.18	0.10	−0.40
	diffusion	−0.75	0.46	−0.34	0.16
	pore size	0.21	0.27	0.18	0.06
	pore density	0.32	0.05	0.12	−0.95
	in vivo degradation	−0.74	0.50	−0.54	−0.01
immune response	inside hydrogel	−0.58	0.57	−0.36	−0.07
	surrounding hydrogel	0.41	0.40	0.49	−0.44

(c)collagen hydrogel		**Enginnered tissue construct**			
		weight	**lumen density**	**lumen area**	**hCD31+**
materials properties	[RGD], [MMP]	0.95	−0.32	0.33	−0.29
	G'	0.24	−0.34	−0.18	0.23
	swelling	−0.02	0.24	0.16	−0.74
	diffusion	−0.66	0.75	−0.39	0.06
	pore size	−0.10	0.62	−0.26	0.33
	pore density	0.23	−0.47	0.24	−0.39
	in vivo degradation	−0.78	0.45	−0.45	−0.32

(c)collagen hydrogel		Enginnered tissue construct			
		weight	lumen density	lumen area	hCD31+
immune response	inside hydrogel	−0.55	0.88	−0.28	−0.31
	surrounding hydrogel	0.29	0.29	0.40	−0.43